The HKU Scholars Hub   The University of Hong Kong   香港大學學術庫

Title	**Susceptibility weighted imaging (SWI) for the assessment of iron loading in the brain of beta-thalassemia major patients**
Author(s)	**Qiu, D; Chan, GC; Chan, Q; Ha, SY; Khong, PL**
Citation	**The 2010 Joint Annual Meeting of ISMRM-ESMRMB, Stockholm, Sweden, 1-7 May 2010.**
Issued Date	**2010**
URL	**http://hdl.handle.net/10722/126013**
Rights	**Creative Commons: Attribution 3.0 Hong Kong License**

Susceptibility weighted imaging (SWI) for the assessment of iron loading in the brain of beta-thalassemia major patients

D. Qiu[1], G. C. Chan[2], Q. Chan[3], S-Y. Ha[2], and P-L. Khong[1]
[1]Diagnostic Radiology, The University of Hong Kong, Hong Kong, China, People's Republic of, [2]Pediatric and Adolescent Medcine, The University of Hong Kong, Hong Kong, China, People's Republic of, [3]Philips Healthcare Hong Kong, Hong Kong, China, People's Republic of

Introduction: Cognitive impairment has been observed in thalassemia patients (1) and it may be related to iron overload. Increased iron deposition was also reported in the basal ganglion regions in thalassemic patients previously. SWI with phase map allows more sensitive detection of iron content in the brain with higher image resolution (2). Therefore, we used SWI to quantify iron store in the brain of thalassemia patients with comparison to age matched normal subjects.

Method: Thirty-four (17 Male) beta-thalassemia major patients and 34 (17 Male) age matched healthy normal volunteers were recruited for the study. The mean/SD of age was 24.4/6.1 and 26.4/4.0 years for the patient and the control groups respectively. MRI scan was performed using a Philips 3T scanner, and included a 3D gradient-echo sequence for SWI (FOV=230mm, Matrix=256x256, Slice thickness = 2mm, TR/TE =16/23ms) and a structural imaging sequence using either MPRAGE or 2D T1 weighted (T1W) technique for anatomical identification and image normalization. The phase image of the SWI sequence was processed to remove background field variation using a standard complex division method (3). All images were normalized to a standard brain template in SPM using the T1W image as a medium, and the mean phase image was created. Region-Of-Interests (ROI) were drawn on the mean phase map and included bilateral caudate nucleus (CN), putamen (PT), globus pallidus (GP), red nucleus (RN), substantia nigra (SN) and dentate nucleus (DN) (Fig 1). The mean phase value (PV) was calculated as the mean value of all non-positive voxels within a ROI as defined above; the restriction to non-positive voxels was imposed to alleviate the dipole effects which induce large positive phase value around regions of

Fig. 1 shows placement of ROIs.

high susceptibility (e.g. caused by high iron density). Lower PV suggests higher iron loading. The left and right phase values were then averaged for further statistical analysis. We established normal range of PV by performing linear regression on the PV for each ROI with gender and age as independent variables in the control group. The expected normal PV for an individual can then be calculated as expectedPV = intercept + gender effect + age * (slope for age effect). The age and gender corrected PV (cPV) was then calculated as cPV = PV- expectedPV. A PV 2.5 times standard deviation (SD) lower than the expected normal PV (i.e. cPV < -2.5*SD) was defined as Low Phase Value (LPV), which suggests iron over-loading; conversely a PV 2.5 times SD higher than the expected normal PV (i.e. cPV > 2.5*SD) was defined as High Phase Value (HPV), which suggests iron under-loading. Pearson's correlation was performed between PV of each ROI with blood ferritin level taken within 2 months before and after the MR scan as well as its average over one year period. ANOVA analysis was performed to compare cPV of each ROI between patients receiving different types of chelation therapy, cPV rather than PV was used in order to control for the confounding effects of potentially different age of subjects receiving different types of chelation therapy.

Results: Qualitatively, SWI was able to show nicely regions of high iron deposition. In some thalassemia cases, high amount of iron deposition was shown as low signal intensity in magnitude image and phase image in regions including the PT and the GP (Fig. 2). With increasing age, PV decreased in the control group in the PT, CN, DN, SN and RN, and the effect reached statistical significance for RN (p =0.016), which is in keeping with the literature of increased iron deposition with older age.

Different patterns of iron loading was observed (Table 1).Out of 34 subjects, 10 had normal PV in all ROIs while 24 had abnormal PV in at least one of the ROIs. Among them, 5 (3 female) patients were categorized as "pure" iron over-loaded as at least one of the ROIs had LPV (Lower Phase Value, see Methods section for definition) while no ROI had HPV (High Phase Value, see Methods section for definition), of whom 1 involved PT, 2 GP, 1 CN and 4 RN; 17 (9 female) patients were categorized as "pure" iron under-loaded as at least one of the ROIs had HPV while none had LPV, of whom 11 involved GP, 8 CN, 4 DN and 5 SN; 2 subjects (both male) had "mixed" findings, one had LPV in GP and HPV in CN, SN and RN, while the other had LPV in DN and HPV in CN.

There was no significant correlation between measures of blood ferritin level and PV of the ROIs.

For iron chelation therapy, 9 received DFO, 7 L1, 14 DFO& L1, and 4 Exjade. ANOVA analysis showed significant difference in cPV between patients with different chelation therapy in CN (p = 0.015) (Fig. 3) and SN (p = 0.036), while there was a trend towards statistical significance for PT (p = 0.075). Post-hoc analysis showed that cPV in CN was significantly higher for L1 compared to DFO (p = 0.02) and Exjade (p = 0.045). Post-hoc analysis also showed significantly higher cPV in SN in patients receiving L1 compared to DFO (p=0.036). Quantitatively, cPV was found to be consistently higher in all other ROIs in patients receiving L1 compared to DFO, suggest L1 being a more effective iron chelation agent.
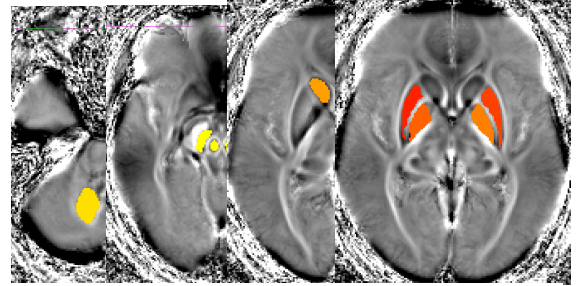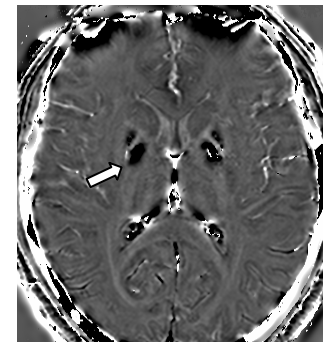

Fig. 2 shows an example of high iron concentration in PT and GP with low signal intensity in the phase map.

	Total # /Female #	PT	GP	CN	DN	SN	RN
Normal	10/5						
Pure overload	5/3	1	2	1	0	0	4
Pure underload	17/9	0	11	8	4	5	0
Mixed	2/0	0	1+	2-	1+	1-	1-

Table 1 shows distribution of patients according their pattern of iron loading in the brain. (See main text for explanation).
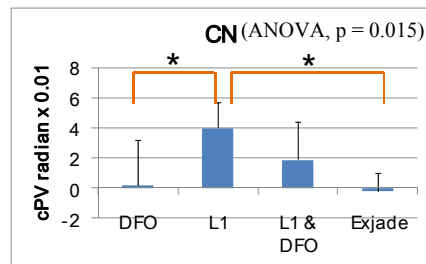

Fig. 3. Significant difference in cPV was found in CN among patients receiving different iron chelation agents (p = 0.015). Post-hoc analysis showed significantly higher cPV in patients receiving L1 compared to DFO (p=0.02) and Exjade (p = 0.045).

Discussion: SWI is sensitive to iron deposition in the brain, which, on the one hand, is nicely visualized as dark areas in magnitude image, and on the other hand, can be quantified using the phase map. Variations in the phase value most likely reflect differences in iron concentration (2). The wide range of phase value among thalassemia suggests that SWI can sensitively capture changes in iron concentration. We found not only patients with high iron loading but also patients with low iron loading. This variation is likely due to the dynamic interactions between the effects of regular blood transfusion and iron chelation therapy. Indeed, we found significant differences in phase value between patients with different iron chelation therapy, prompting further research on the best chelation therapy for a given individual. While over-loading of iron content is generally recognized as neuro-toxic due to the oxidative effects, it is not clear of the effect of lower iron concentration at cellular level or the level of overall cognitive ability although there are evidences that iron is important for the proliferation of cells. In conclusion, SWI is sensitive in measuring iron concentration in the brain and provides a valuable tool for iron assessment both for clinical trials and for individual evaluation.

References: *1.* Monastero R, et al. Acta neurologica scandinavica.2000; 102:162-168. *2.* OGG RJ, et al. Magn Reson Imaging.1999; 17:1141-1148. *3.* Wang Y, et al. 2000. J Magn Reson Imaging. 2000; 12:661–670